13 Path Integrals and Reference Systems

Alexander Lichtenstein
I. Institut für Theoretische Physik
Universität Hamburg, 22607 Hamburg, Germany

Contents

E. Pavarini, E. Koch, A. Lichtenstein, and D. Vollhardt (eds.)
Understanding Correlated Materials with DMFT
Modeling and Simulation Vol. 15
Forschungszentrum Jülich, 2025, ISBN 978-3-95806-813-1
http://www.cond-mat.de/events/correl25

1 Idea of reference systems

In this lecture we give an introduction to the theoretical description of correlated electron systems within a path integral approach. First, numerically exact calculations of interacting path integrals via continuous-time Quantum Monte Carlo methods (QMC) [1] are revisited. Next, the strong-coupling path-integral Dual-Fermion (DF) expansion around optimally chosen reference system is presented. Finally, the response of the single-band, hole doped t-t' Hubbard model to an external superconducting d-wave field is discussed.

The most well known reference system scheme in quantum material science is related to the celebrated Density Functional Theory (DFT) and their Local Density Approximation (LDA). In this case a homogeneous electron gas with constant external potential and the same Coulomb electron-electron interactions have been solved (see Fig. 1), and this results served as the reference for inhomogeneous electron crystals via a simple LDA ansatz. Such a reference system is exactly solvable via a diffusion quantum Monte Carlo scheme for the ground state energy as a function of the electron density [2]. On other hand, the Dynamical Mean-Field Theory (DMFT) [3] for strongly interacting fermionic systems is based on the self-consistent solutions of an effective impurity reference system (Fig. 1). For realistic multi-orbital systems such a scheme uses a fermionic impurity bath with frequency dependent hybridization function Δ_ω for the correlated part of electrons described by the family of DFT+DMFT approaches [4]. The DMFT scheme becomes exact in the limit of infinite lattice dimension [5].

At finite lattice dimension one can start from the DMFT reference system and use different perturbation schemes for non-local correlation effects [3]. The frequency dependent effective impurity DMFT problem nowadays can be efficiently solved within the continuous time quantum Monte Carlo (CT-QMC) scheme [1]. Therefore the perturbation theory needs to be formulated within the action path integral formalism. We discuss here a general way to include correlations beyond the interacting reference system [6] which are based on the strong coupling dual-fermion path-integral formalism [7]. In the case of additional non-local interactions, the so-called GW+DMFT scheme and impurity reference systems with fermionic and bosonic bathes can be used and so-called dual-boson approach for non-local correlations [6].

For DMFT an effective impurity model, designed to the problem of correlated materials, serves as the reference system, see Fig. 1. Since the zeroth order of such a non-local perturbative expansion coincides with the DMFT problem, we already have an interacting system from the beginning. Moreover, the perturbation is momentum and frequency dependent, so we are forced to replace the Hamiltonian approach by an actions path-integral formalism. Note that the fermion path integral can be used also to formulate the DMFT problem [3, 7]. The dual-fermion approach is not necessarily bound to a specific starting point and can also be used for correlated lattice reference system.

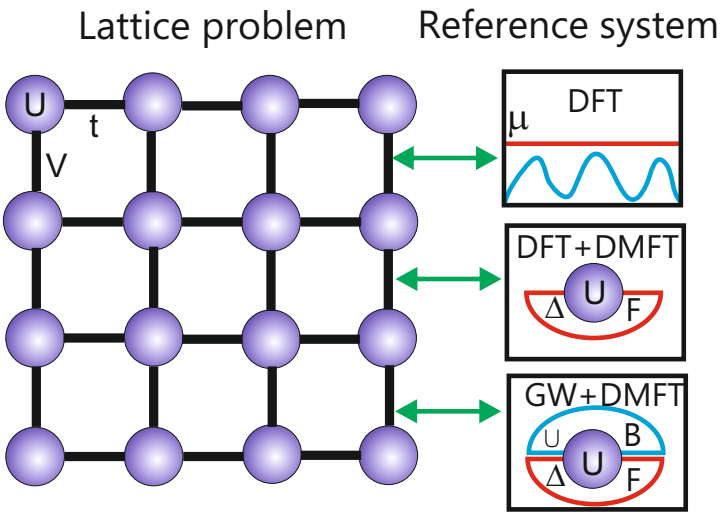

Fig. 1: *Schematic representation of reference systems in many-body approaches to lattice-fermion models: (i) Density-functional theory (DFT) with the interacting homogeneous electron gas as a reference system, defined by a constant external potential μ. (ii) Dynamical mean-field theory (DMFT) with an effective impurity problem as a reference system, defined by a fermionic bath with hybridization function Δ. (iii) GW+DMFT with a correlated atom in a fermionic (Δ) and bosonic (Λ) bathes describes effects of frequency-dependent screened long-range Coulomb (V) interactions.*

2 Path integral for correlated lattice model

Let us consider a general interacting lattice fermion model in d-dimensions described by following Hamiltonian $\hat{H} = \hat{H}_0 + \hat{V}_{\text{int}}$ in second quantization form

$$\hat{H} = \sum_{12} t_{12}\, \hat{c}_1^\dagger \hat{c}_2 + \frac{1}{2} \sum_{1234} V_{1234}\, \hat{c}_1^\dagger \hat{c}_2^\dagger \hat{c}_4 \hat{c}_3 \,. \tag{1}$$

In order to keep the notation simple, it is useful to introduce a combined index for the orthonormal Wannier basis set: $|1\rangle \equiv |r, m, \sigma\rangle$ with site r, orbital m and spin σ. The one electron hopping matrix elements reads $t_{12} = \langle 1|\hat{H}_0|2\rangle$ and general interaction tensor is $V_{1234} = \langle 12|\hat{V}_{\text{int}}|34\rangle$. For multiorbital systems it is useful to introduce the fully antisymmetric interactions vertex: $U_{1234} = V_{1234} - V_{1243}$ with an additional factor $\frac{1}{2}$ in the last sum of Eq. (1). We use atomic units with $\{m, e, \hbar, k_B\} = 1$. In the path-integral formalism (see Appendix A), the equilibrium partition function of a general fermionic lattice system with Hamiltonian Eq. (1) and inverse temperature $\beta = 1/T$ can be written in the form of a functional integral in d+1 dimensions over Grassmann variables $[c^*, c]$ (corresponding to the original operators $[\hat{c}^\dagger, \hat{c}]$)

$$Z = \int \mathcal{D}[c^*, c]\, e^{-S[c^*, c]} \tag{2}$$

with Euclidean action for imaginary time $\tau = it$

$$S[c^*, c] = -\sum_{1,2} c_1^*\, \mathcal{G}_{12}^{-1}\, c_2 + \frac{1}{4} \sum_{1234} U_{1234}\, c_1^* c_2^* c_4 c_3 \,, \tag{3}$$

with inverse bare Green function matrix

$$\mathcal{G}_{12}^{-1} = -\partial_\tau - t_{12}\,, \tag{4}$$

where the Grassmann variable index means $|1\rangle \equiv |r, m, \sigma, \tau\rangle$ and following the definition of "summation" over continuous imaginary time τ in the $[0, \beta]$ interval

$$\sum_1 \{\cdots\} \equiv \sum_{i,m,\sigma} \int_0^\beta d\tau\, \{\cdots\}\,. \tag{5}$$

All single-particle effects in solids can be described with the help of the one-electron Green function for interacting fermion systems with Hamiltonian in Eq. (1), which may be represented as the following path-integral over action in Eq. (3)

$$G_{12} = -\langle c_1 c_2^* \rangle_S = -\frac{1}{Z}\int \mathcal{D}[c^*, c]\, c_1 c_2^*\, e^{-S[c^*,c]}\,. \tag{6}$$

Note, that in the functional integral of Eq. (6) the anti-commuting Grassmann variables are automatically "ordering" in the imaginary times and one does not need to introduce the "time-ordering" operator in the definition of Green function.

We will discuss in this chapter different methods for numerical "path-integrations" of Eq. (6) which are all related to different flavors of the continuous time (CT) quantum Monte Carlo (QMC) scheme. The first approach, namely Diagrammatic Monte Carlo (DiagMC) was developed for bosonic systems [8] and is related to a QMC-summation of Feynman diagrams with an important sampling strategy. For fermionic systems two successful versions of CT-QMC exist and are related with the interaction expansion (CT-INT) [9] and the hybridization expansion (CT-HYB) family of impurity solvers [1]. Finally, the lattice version of the CT-INT scheme for the one-particle irreducible self-energy with only connected Feynman diagrams, the so called CDet approach was developed recently [10].

The main problem with calculations of the path integral in Eq. (6) is related with the fact that the only known answers refer to non-interacting system (see Appendix A). The interaction expansion (CT-INT) continuous-time quantum Monte Carlo algorithm for fermions is based on a formal series expansion for the partition function (3) in the U-terms of the action in Eq. (3) [9]. In a schematic form we have

$$Z = \int \mathcal{D}[c^*, c]\, e^{-S_0[c^*,c]} \sum_{k=0}^{\infty} \sum_{1234} \frac{(-1)^k}{4^k k!} \int_0^\beta d\tau_1 \cdots d\tau_k \big(U_{1234}\, c_1^* c_2^* c_4 c_3\big)^k \tag{7}$$

where S_0 is the Gaussian part of the action (3) related with the bare Green function $\mathcal{G}_{12}$. In this case we can integrate out the fermionic path integral in Eq. (7) for each k-th terms and get a $k\times k$ determinant of bare Green functions of two spin-projections of $\mathcal{G}^\sigma$ in the paramagnetic state (the factor $k!$ is cancelled for new time integration area)

$$Z = Z_0 \sum_{k=0}^{\infty} \sum_{1234} \big(-\frac{1}{2} U_{1234}\big)^k \int_0^\beta d\tau_1 \cdots \int_{\tau_{k-1}}^\beta d\tau_k\, \det \mathcal{G}^\uparrow_{k(31)} * \det \mathcal{G}^\downarrow_{k(42)} \equiv \sum_{\mathcal{C}} s(\mathcal{C}) W(\mathcal{C}), \tag{8}$$

where the $k\times k$ matrix of bare Green function is defined as

$$\hat{\mathcal{G}}_k = \begin{pmatrix} \mathcal{G}_{11} & \mathcal{G}_{12} & \cdots & \mathcal{G}_{1k} \\ \mathcal{G}_{21} & \mathcal{G}_{22} & \cdots & \mathcal{G}_{2k} \\ \vdots & \vdots & \ddots & \vdots \\ \mathcal{G}_{k1} & \mathcal{G}_{k2} & \cdots & \mathcal{G}_{kk} \end{pmatrix}, \tag{9}$$

and the indices (31) and (42) in Eq. (8) just indicates how pairs of space-orbital-time indices are connected to the corresponding indices of the interaction vertex U_{1234} and is "repeated" k-times to couple $\hat{\mathcal{G}}_k^{\uparrow}$ and $\hat{\mathcal{G}}_k^{\downarrow}$ matrices to all k-vertices: $(U_{1234})^k$. In order to overcome a trivial sign problem related with the factor $(-U)^k$ one uses a particle-hole transformation related with so-called α-shift [9]. The CT-INT scheme is performed by Monte Carlo importance sampling in the space $\mathcal{C}$ of $k\times k$ fermionic determinants with the probability defined by absolute value of the full expression in Eq. (7) under sum and integral. We also introduce the "sign" $s(\mathcal{C})$ of the product of two determinants which is not always positive. This is the reason for the so-called QMC fermionic sign problem which plays an important role in all quantum Monte Carlo simulations. One can rewrite Eq. (7) as $Z = \big\langle s(\mathcal{C})\big\rangle_{MC}$ with the average over Monte Carlo runs with corresponding probabilities. Note, that for a half-filled particle-hole symmetric Hubbard-like model the product of two fermionic determinants is always positive and there is no sign problem. The probability to change from k-th to $k{+}1$-th order in the Metropolis algorithm is related with ratio of the fermionic determinants [9]

$$P(k \to k{+}1) = \min\left(1, \frac{\beta U}{k{+}1} \prod_{\sigma} \frac{\det \mathcal{G}_{k+1}^{\sigma}}{\det \mathcal{G}_{k}^{\sigma}}\right). \tag{10}$$

The optimal order of k-perturbation, which corresponds to the maximum of the distribution function of the fermionic determinants size for a cluster of N-sites is of the order $k_{\text{opt}} \sim \beta N U$ [9]. We can see that for finite fermionic system at non-zero temperature ($\beta \neq \infty$) the CT-INT "perturbation" k-series is convergent (Fig. 2).

The simplest way to find the expressions for the Green function and other correlation functions uses functional derivatives of the action Eq. (3) in an external Grassmann fields (J^*, J)

$$S[J^*, J] = S[c^*, c] + \sum_i (c_i^* J_i + J_i^* c_i)\,. \tag{11}$$

In this case we have:

$$G_{ij} = -\langle c_i c_j^* \rangle_S = \frac{1}{Z} \frac{\delta^2 S[J^*, J]}{\delta J_i^* \delta J_j} \bigg|_{J^*=J=0}. \tag{12}$$

Using Eq. (8) we can write the Green function schematically as

$$G_{ij}^{\sigma} = \frac{1}{Z} \big\langle s(\mathcal{C}) \det \mathcal{G}_{k+(ij)}^{\sigma} / \det \mathcal{G}_{k}^{\sigma} \big\rangle_{kMC}\,, \tag{13}$$

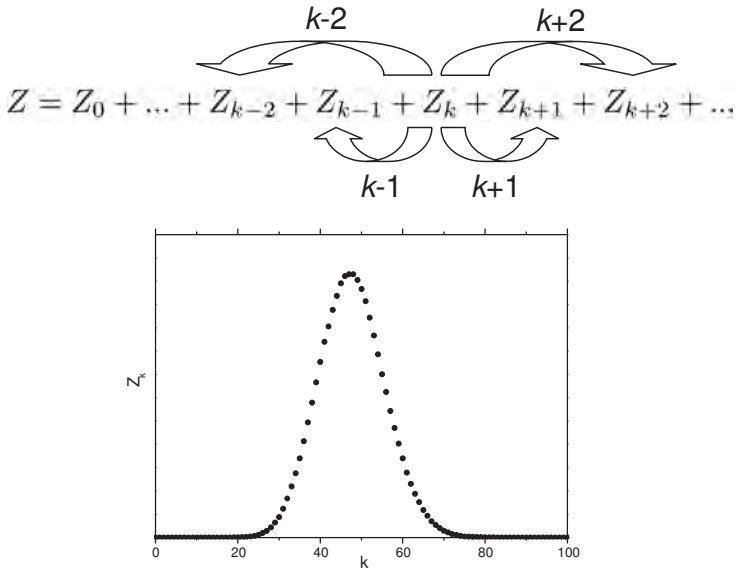

Fig. 2: *A random walk in the space of fermionic determinants Z_k according to the perturbation series expansion Eq.(8) and an example of the histogram for the perturbation order Z_k in Eq.(10). For single-particle properties it is enough to use only $k \mapsto k\pm1$ moves. For two-particle properties it is useful to include also $k \mapsto k\pm2$ moves.*

where $\hat{\mathcal{G}}_{k+(ij)}$ is the $(k+1)\times(k+1)$ matrix

$$\hat{\mathcal{G}}_{k+(ij)} = \begin{pmatrix} \mathcal{G}_{11} & \mathcal{G}_{12} & \cdots & \mathcal{G}_{1k} & \mathcal{G}_{1j} \\ \mathcal{G}_{21} & \mathcal{G}_{22} & \cdots & \mathcal{G}_{2k} & \mathcal{G}_{2j} \\ \vdots & \vdots & \ddots & \vdots & \vdots \\ \mathcal{G}_{k1} & \mathcal{G}_{k2} & \cdots & \mathcal{G}_{kk} & \mathcal{G}_{kj} \\ \mathcal{G}_{i1} & \mathcal{G}_{i2} & \cdots & \mathcal{G}_{ik} & \mathcal{G}_{ij} \end{pmatrix}, \tag{14}$$

and Monte Carlo just averages over the k-space of fermionic determinants. The ratio of the two determinants in Eq. (13) we can calculate exactly [9] and the final CT-INT expression reads (skip the same index σ)

$$G_{ij} = \mathcal{G}_{ij} - \frac{1}{Z}\,\mathcal{G}_{ii'} * \left\langle s(\mathcal{C})\,\left[\mathcal{G}_k^{-1}\right]_{i'j'} \right\rangle_{kMC} * \mathcal{G}_{j'j}\,, \tag{15}$$

The CT-INT scheme gives a very stable and accurate results for the Green function for small clusters, but for bigger systems the average size of the determinants in Eq. (13) becomes prohibitively large. Note that $\det \mathcal{G}_k^\sigma$ together with the interaction vertices U^k represents $k!$ Feynman diagrams both connected and disconnected. It is known from the "linked cluster theorem" [11] that the disconnected diagrams are exactly cancelled with the denominator Z. Therefore, the most efficient way to obtain the Green function is related with a lattice diagrammatic Monte Carlo scheme within the connected determinants (CDet) approach [10]. The main idea of the CDet method is related with the fact that one can iteratively subtract all non-connected diagrams during the Monte Carlo move in the space of fermionic determinants. These disconnected Feynman diagrams can be represented as subset $\mathcal{S}\subsetneq\mathcal{C}$ of connected diagrams of the lower order times all remaining diagrams. We can represent schematically the Green function

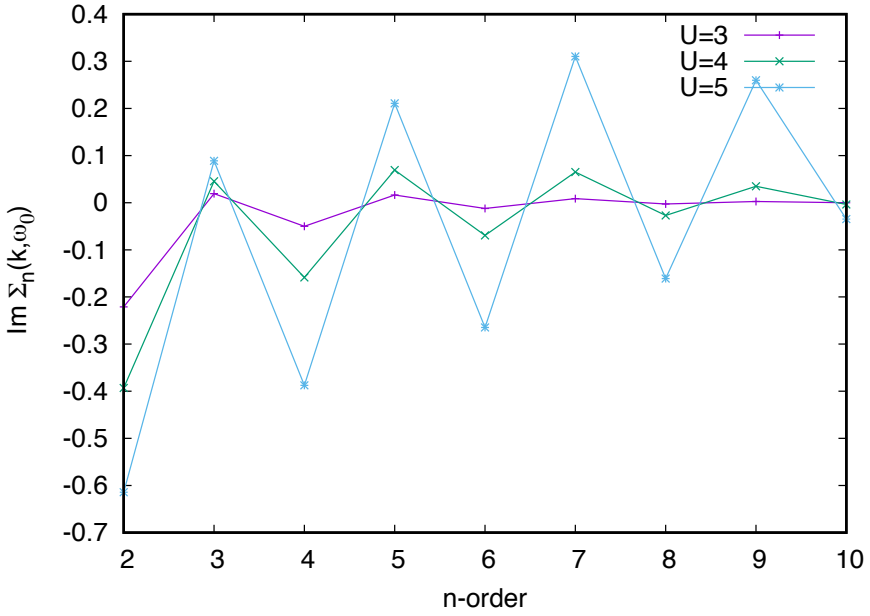

Fig. 3: *Contribution of different perturbation orders to the imaginary part of the self-energy* $\Sigma(\mathbf{k},\omega_0) = \sum_n \Sigma_n(\mathbf{k},\omega_0)$ *for* $\mathbf{k} = (\pi, 0)$, $\beta = 5$, $t'/t = -0.3$, $N = 0.85$ *with increasing interaction strength* U *in the* 64×64 *Hubbard lattice within the CDet scheme [12].*

calculations within a CDet Monte Carlo step in the space of $\mathcal{C}$ configuration as

$$G(\mathcal{C}) = \det \mathcal{G}(\mathcal{C}) - \sum_{\mathcal{S}\subsetneq\mathcal{C}} G(\mathcal{S}) \det \mathcal{G}\big(\mathcal{C}\backslash\mathcal{S}\big) \,. \tag{16}$$

This is the most "time-consuming" procedure to get rid of all disconnected diagrams for the given k-order of determinants using all smaller rank determinants on the right-hand side of Eq. (16). The great progress of the CDet approach compared with DiagMC allowed to calculate up to 12-th order in the U^k perturbation series in Eq. (8) for the Hubbard model for very large systems in the thermodynamic limit. It is also possible to formulate iterative series of connected Feynman diagram directly for a self-energy similar to Eq. (16), which reduces the computational cost for such one-particle irreducible schemes. Moreover, the sign-problem in lattice QMC turns to a "sign-blessing" which can help in averaging to zero all higher diagrammatic contributions that are not calculated in the CDet scheme [10]. Investigations of pseudogap phase for a one-band Hubbard model of doped cuprates [12] show the high accuracy of such path-integral scheme. For young researchers there is the very useful possibility to test the CDet code included in the Supplementary Materials of [12].

The main problem of the CDet scheme is the poor convergence of series $\Sigma = \sum_k U^k \Sigma_k$ which for large $U{>}5t$ start to diverge (see Fig. 3) and one needs to use a resummation scheme from conformal field theory. Nevertheless, for the part of phase space (U, β, n) where the CDet scheme is converged (e.g. for large temperature, $\beta{=}5$), this method can be considerd as numerically exact solution of correlated lattice problem. As example of CDet results [12] we show in Fig. 4 the spectral function of Hubbard model for a large system of of 64×64 sites with strong interactions. One can see the complicated electronic structure of interacting fermions with the pseudogap feature at the $X{=}(\pi, 0)$ point and the antiferromagnetic shadow bands.

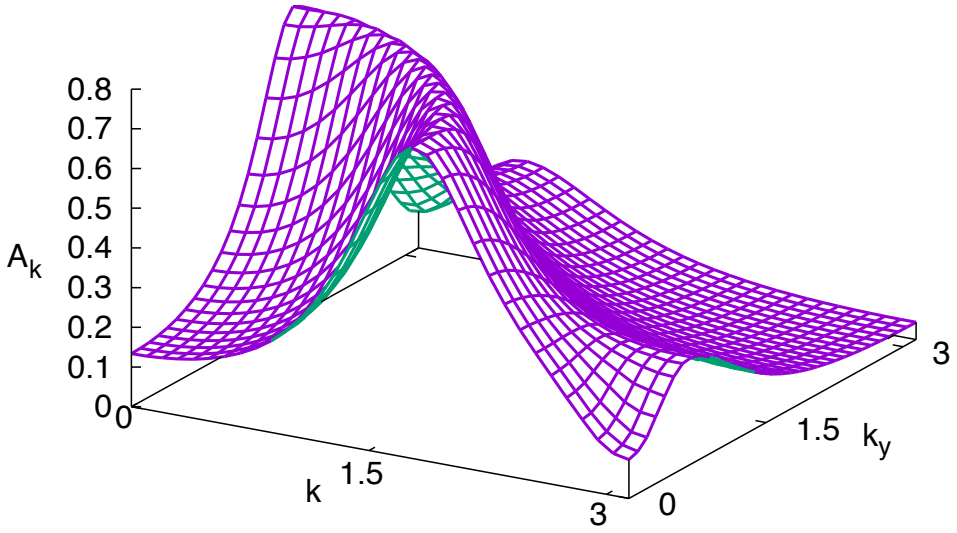

Fig. 4: *Spectral function* $A_k{=}-\operatorname{Im} G(\mathbf{k},\omega_0)$ *at the lowest Matsubara frequency* $\omega_0{=}\pi/\beta$ *for* $\beta{=}5$, $N{=}0.85$, $t'/t{=}-0.3$, $U{=}5$ *in the* $64{\times}64$ *Hubbard lattice within the CDet scheme [12].*

We now turn to a different route to tackle the "sign problem" in the determinant lattice QMC scheme and design a strong-coupling perturbative solution for a general Hubbard model. The starting point is related to the "reference system" idea [13]. The choice of a single-site approximation like dynamical mean-field theory [3] as the reference system leads to the dual fermion technique [7].

3 Expansion around reference system

We discuss a general path-integral method for expansions around arbitrary reference systems. In fact, the CT-INT scheme (see Eq. (8)) can be considered as a special case of the reference system approach which is just the free fermion case, described by the Gaussian quadratic part $\mathcal{G}_{12}$ of the action in Eq. (3). In this case the path-integral expansion is particularly simple and coincides with the weak coupling perturbation which is described by the series of fermionic determinants built from the bare propagators $\mathcal{G}_{12}$. Now we considered a more general case, where the reference system consists of interacting fermions. We start with the simple case of a Hubbard-like model, where the interaction strength U is fixed to be the same for the reference and target systems, and only small changes in the one-electron part will be considered in lowest orders of the path-integral expansion. In fact this approach has many commons details with the Dual-Fermion (DF) lattice expansion around the local DMFT starting point [7]. In a more general case, when the interactions strength is different in reference and system, one should use a so-called Dual-Boson theory [6].

We consider the simple case of interacting fermions on a lattice within the single band Hubbard model, defined by the Hamiltonian

$$\hat{H}_\alpha = -\sum_{i,j,\sigma} t_{ij}^{\alpha}\, \hat{c}^{\dagger}_{i\sigma}\hat{c}_{j\sigma} + \sum_i U\left(\hat{n}_{i\uparrow}-\frac{1}{2}\right)\left(\hat{n}_{i\downarrow}-\frac{1}{2}\right) \tag{17}$$

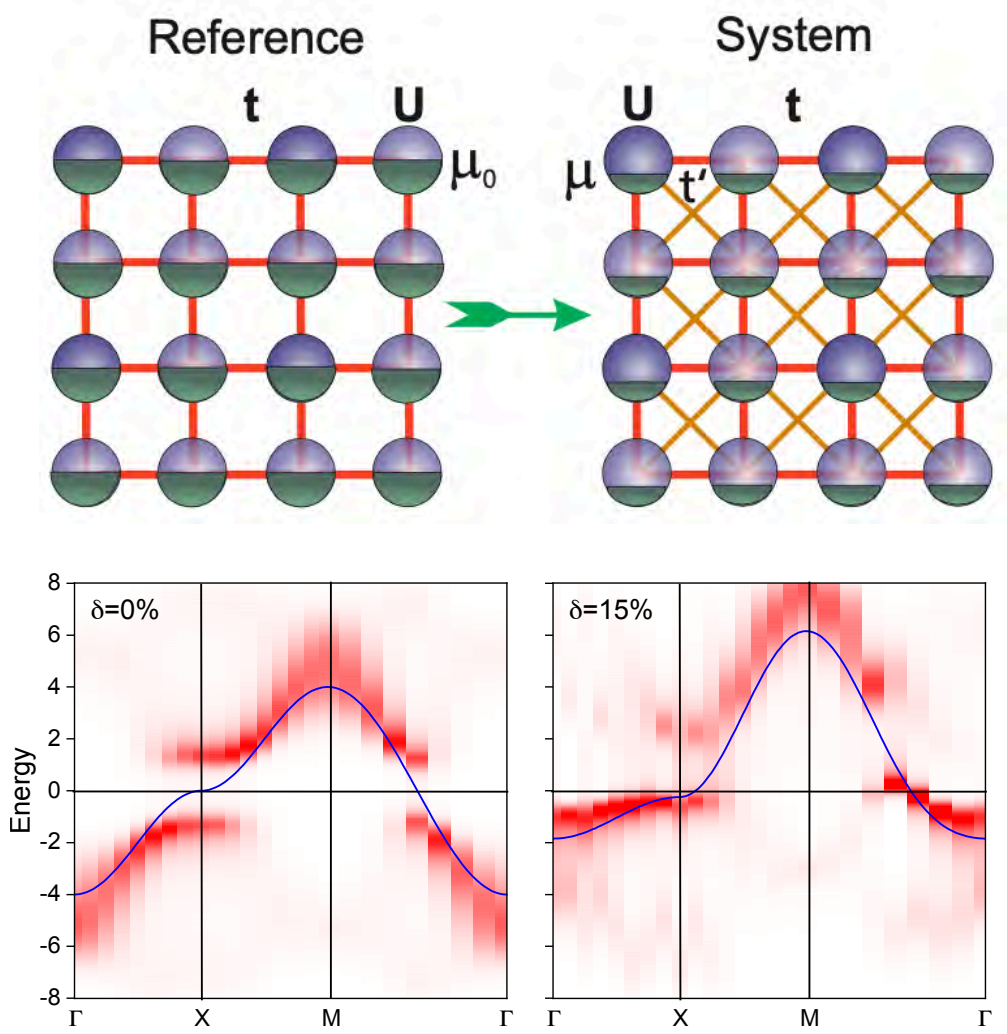

Fig. 5: *Schematic representation of a half-filled reference system (left) for the doped* $(t$-t'-$U)$ *square lattice (right). Bottom: Electronic spectral function of the* t-t' *Hubbard model calculated for* U=5.6 *at* β=5 *relative to the chemical potential together with the non-interacting dispersions (blue line). The reference results are obtained for the half-filled particle-hole symmetric case* t'=0*, (left panel), the DF-QMC results for* δ=15% *hole doping with* t'=−0.3 *(right).*

where t_{ij} are the hopping matrix elements including the chemical potential μ in the diagonal

$$t_{ij}^{\alpha} = \begin{cases} t & \text{if } i \text{ and } j \text{ are nearest neighbors,} \\ \alpha t' & \text{if } i \text{ and } j \text{ are next nearest neighbors,} \\ \alpha\mu & \text{if } i = j, \\ 0 & \text{otherwise,} \end{cases} \tag{18}$$

where $\hat{n}_{i\sigma} = \hat{c}_{i\sigma}^{\dagger}\hat{c}_{i\sigma}$. We use a "scaling" parameter α, which distinguishes the reference system H_0 for α=0 corresponding to the half-filled Hubbard model (μ_0=0) with only nearest neighbors hopping (t_0'=0) from the final system H_1 for α=1 with given μ and t'. Note that longer-range hoping parameters can be trivially included in the present formalism similarly to t'.
The reference system now corresponds to the half-filled (μ_0=0) particle-hole symmetric (t_0'=0) case (Fig. 5) where lattice Monte Carlo has no sign problem and the numerically exact solution

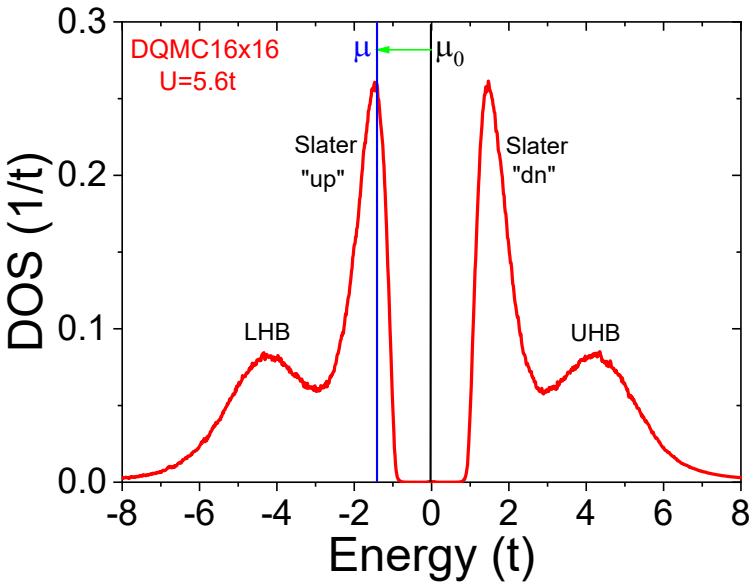

Fig. 6: *The DOS of the normal state at* β=10 *for the reference system corresponding to a* 16×16 *lattice with* t=1, U=5.6, t'=0, *and* μ=0 *using the DQMC scheme and the MaxEnt analytical continuation to real energy.*

for any practical value of U is possible within a broad range of temperatures [14]. Then we apply the lattice dual fermion QMC perturbation theory [7, 13, 15] to find the first-order perturbative corrections in μ and t'. To this aim, it is sufficient to calculate the two-particle Green function or, equivalently, the four-leg vertex, which can be done accurately enough with continuous time quantum Monte Carlo. Our reference system already has the main correlation effects in the lattice and shows the characteristic "four-peak" structure [16] with the high-energy "lower" and "upper" Hubbard bands at $E \simeq \pm 5t$ as well as the two "Slater" peaks close to the Mott gap at $E \simeq \pm 2t$ related to the "band-like" antiferromagnetic splitting of "spin-up" and "spin-down" electrons for a particular local site, which can be seen in Fig. 6. This is an ideal reference point to investigate the effects of doping and breaking of partial-hole symmetry by a particular sign of t'. After the dual-fermion perturbation approach, which we will discuss, the correlated metallic states appeared on Fig. 5 (right panel). The results for the strong-coupling case (U=5.6t) with practically interesting values of the chemical potential and next-nearest-neighbor hopping corresponding to cuprate superconductors indicate the formation of a pseudogap and the nodal-antinodal dichotomy (that is, well-defined quasiparticles in the nodal part of the Fermi surface and strong quasiparticle damping for the antinodal part) which gives this approximation a perspective for practical applications.

We start with a most general definition of a perturbation matrix related to the difference of one-electron part of action

$$\tilde{t} = \mathcal{G}_0^{-1} - \mathcal{G}_1^{-1} \,. \tag{19}$$

This can apply to a general case of a system in an external fermionic bath and therefore defines our perturbation $\tilde{t}$ in terms of the one-electron part of reference-system action. In case of a pure Hamiltonian systems, our perturbation is related with the difference of the effective hopping

matrix t_{ij}^{α} and in $\mathbf{k}$-space is equal to

$$\tilde{t}_{\mathbf{k}} = -4t' \cos k_x \cos k_y - \mu \,. \tag{20}$$

In order to formulate an expansion around reference action S_0 we express the connection to the final action $S \equiv S_1$ with the same local interaction in the following form

$$S[c^*, c] = S_0[c^*, c] + \sum_{12} c_1^* \, \tilde{t}_{12} \, c_2 \,. \tag{21}$$

The main idea of the dual fermion transformation is the change of variables (similar to the Fourier transform) from the strongly correlated fermions (c^*, c) in Eq. (3) to the weakly correlated "dual" Grassmann fields (d^*, d) in the path integral representation for the partition function in Eq. (21), followed by a simple perturbation treatment. The new variables were introduced through the following Hubbard-Stratonovich transformation with the perturbation matrix $\tilde{t}_{12}$ in real-space (the Einstein summation convention over repeated indices is assumed)

$$e^{-c_1^* \, \tilde{t}_{12} \, c_2} = Z_t \int \mathcal{D}\,[d^*, d] \, e^{d_1^* \, \tilde{t}_{12}^{-1} \, d_2 + d_1^* c_1 + c_1^* d_1} \tag{22}$$

with $Z_t = \det(-\tilde{t})$ and we always assume the matrix inversion: $\tilde{t}_{12}^{-1} \equiv (\tilde{t}^{-1})_{12}$. Using this transformation, the lattice partition function becomes

$$Z = Z_0 Z_t \int \mathcal{D}[d^*, d] \, e^{d_1^* \, \tilde{t}_{12}^{-1} \, d_2} \, \left\langle e^{d_1^* c_1 + c_1^* d_1} \right\rangle_0 \tag{23}$$

with the standard definition of average over S_0

$$\langle \cdots \rangle_0 = \frac{1}{Z_0} \int \mathcal{D}[c^*, c] \cdots e^{-S_0[c^*, c]}. \tag{24}$$

Now we can integrated out the c^*, c fermions and show that the average over S_0 can be rewritten in the form of a "cumulant expansion" [17] or connected correlators $\langle \cdots \rangle_{0c}$

$$\left\langle e^{d_1^* c_1 + c_1^* d_1} \right\rangle_0 = \exp \left[\sum_{n=1}^{\infty} \frac{(-1)^n}{(n!)^2} \gamma^{(2n)}_{1 \cdots n, n' \cdots 1'} d_1^* \cdots d_n^* d_{n'} \cdots d_{1'} \right] \tag{25}$$

with cumulants or connected correlators for the reference system which can be calculated within the QMC

$$\gamma^{(2n)}_{1 \cdots n, n' \cdots 1'} = (-1)^n \left\langle c_1 \cdots c_n c^*_{n'} \cdots c^*_{1'} \right\rangle_{0c}. \tag{26}$$

We can write the effective action for the "dual fermions" $\tilde{S}[d^*, d]$ in the lowest order approximation for the dual interaction [15]. The first term in the cumulant expansion in Eq. (25) with $n = 1$ or $\gamma^{(2)}_{11'}$ which is bilinear over $[d_1^* \, , d_2]$ the Grassmann variables, corresponds to the exact Green function of reference system

$$\gamma^{(2)}_{11'} \equiv g_{11'} = -\langle c_1 c^*_{1'} \rangle_0 = -\frac{1}{Z_0} \int \mathcal{D}[c^*, c] \, c_1 c_2^* \, e^{-S_0[c^*, c]}. \tag{27}$$

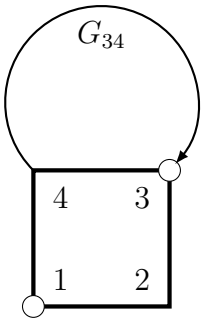

Fig. 7: *Feynman diagram for the first order dual fermion perturbation for the self-energy $\tilde{\Sigma}_{12}$: the line represents the non-local dual Green function $\tilde{G}_{43}$, the box the two-particle vertex γ_{1234}.*

Note, that all correlators of the "reference system" will be written with the small letters. Together with the term $\tilde{t}^{-1}_{12}$ in Eq. (23) this gives a bare Green function for the dual fermions

$$\tilde{G}^0_{12} = \left[\, \tilde{t}^{-1} - \hat{g} \,\right]^{-1}_{12} . \tag{28}$$

The second term in the cumulant expansion in Eq. (25) with $n{=}2$ corresponds to $\gamma^{(4)}_{122'1'}$ which is biquadratic over the $[d^*_1\,, d_2]$ Grassmann variables, and gives an effective two-particle interaction among the dual-fermions.The corresponding connected four-point vertex has the following form (we skip the "(4)" abbreviation)

$$\gamma_{122'1'} = \langle c_1 c_2 c^*_{2'} c^*_{1'} \rangle_0 - \langle c_1 c^*_{1'} \rangle_0 \langle c_2 c^*_{2'} \rangle_0 + \langle c_1 c^*_{2'} \rangle_0 \langle c_2 c^*_{1'} \rangle_0 \tag{29}$$

with four points correlator or two-particle Green function for the reference system

$$\langle c_1 c_2 c^*_3 c^*_4 \rangle_0 = \frac{1}{Z_0} \int \mathcal{D}[c^*, c]\; c_1 c_2 c^*_3 c^*_4 \; e^{-S_0[c^*,c]}. \tag{30}$$

Finally the dual-fermion action in the two-particle approximation has the following form

$$\tilde{S}[d^*, d] = -\sum_{12} d^*_1 \; (\tilde{G}^0)^{-1}_{12} \; d_2 + \frac{1}{4} \sum_{1234} \gamma_{1234} \, d^*_1 d^*_2 d_4 d_3. \tag{31}$$

Note, the effective interaction term for anti-commuting Grassmann variables has the same form as for the standard antisymmetric Coulomb interactions (Eq. (3)). We have shown, that the dual "Fourier" trick transforms strongly correlated fermions with large U_{1234} interactions to weakly correlated dual fermions with effective interactions γ_{1234} which are defined by the screened fully connected two-particle vertex of the reference system. The first order correction to the dual self-energy is given by the diagram shown in Fig. 7 and can be calculated for a large system using the QMC-scheme

$$\tilde{\Sigma}^{(1)}_{12} = \sum_{s-QMC} \sum_{3,4} \gamma^d_{1324}(s) \, \tilde{G}^0_{43} \,, \tag{32}$$

where the density vertex reads

$$\gamma^d_{1234} = \gamma^{\uparrow\uparrow\uparrow\uparrow}_{1234} + \gamma^{\uparrow\uparrow\downarrow\downarrow}_{1234} \,. \tag{33}$$

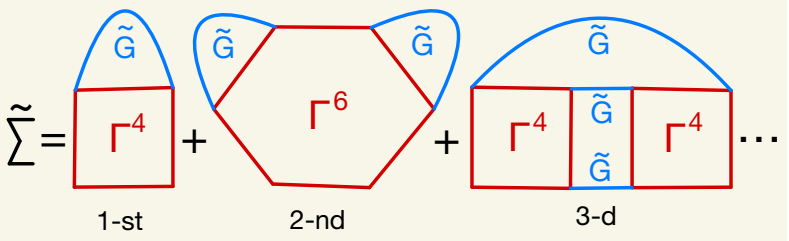

Fig. 8: *Diagrammatic series for the dual self-energy up to the 3-rd order in $\tilde{G}$.*

The main trick for practical computations of large systems is related with the possibility to "factorize" the complicated vertex γ_{1234} inside the stochastic DQMC process with $\{s\}$-auxiliary fields or the CT-INT scheme with stochastic sampling of interaction order expansion $\{s\}$, using the Wick-theorem

$$\gamma_{1234}(s) \equiv \langle c_1 c_2 c_3^* c_4^* \rangle_s = \langle c_1 c_4^* \rangle_s \langle c_2 c_3^* \rangle_s - \langle c_1 c_3^* \rangle_s \langle c_2 c_4^* \rangle_s \,. \tag{34}$$

Finally, one needs to find an exact relationship between the dual and real Green functions [7]. We make variation of $\ln Z$ in Eq.(23) and Eqs.(2, 21) with respect to $\tilde{t}$

$$G_{12} = \frac{\delta \ln Z}{\delta \tilde{t}_{21}} = -\tilde{t}^{-1}_{12} + \tilde{t}^{-1}_{13} \tilde{G}_{34} \tilde{t}^{-1}_{42} \,. \tag{35}$$

Using the definition of the exact dual Green function $\tilde{G}^{-1} = \tilde{G}_0^{-1} - \tilde{\Sigma}$ we can get the expression for the real Green function

$$G_{12} = \left(\left(g + \tilde{\Sigma} \right)^{-1} - \tilde{t} \right)^{-1}_{12} , \tag{36}$$

which means that the dual self-energy has meaning of effective T-matrix term.

The Dual Fermion transformation allowed us to use arbitrary reference systems and transform the strongly correlated lattice fermion problem to an effective action of weakly coupled dual quasi-particles. In this case even the lowest order approximation can give already reasonable results. The exact diagrammatic series for the dual self-energy is presented in Fig. 8. The second order diagram in $\tilde{G}$ which includes $\gamma^{(6)}$ is local within the cluster and can be calculated with a similar QMC scheme. The 3-rd order correction contains two $\gamma^{(4)}$ vertices and it is not easy to sample inside a QMC run. One may compare second order contributions to $\tilde{\Sigma}$ with the fist one and conclude on the convergence of the DF-series.

We can establish also a connection of the DF-formalism with the DMFT approximation: in this case we choose the reference system as an impurity system defined by a frequency dependent hybridization function Δ_ω so that $\tilde{t} = t - \Delta_\omega$. Moreover, all vertices for such a DF-theory will be local and the first non-local contribution to $\tilde{\Sigma}$ will be the 3-rd order diagram in Fig. 8. We can eliminate all local contributions (e.g. fist two diagrams in Fig. 8) if we chose Δ_ω such that $\tilde{G}^0_{loc} = 0$ or using the $\mathbf{k}$-space: $\sum_{\mathbf{k}} \left[\tilde{t}^{-1}_{\mathbf{k}} - g_\omega \right]^{-1} = 0$. Since the impurity Matsubara Green function $g_\omega \neq 0$, we can rewrite this condition as

$$g_\omega = \sum_{\mathbf{k}} \left[g^{-1}_\omega + \Delta_\omega - t_{\mathbf{k}} \right]^{-1} , \tag{37}$$

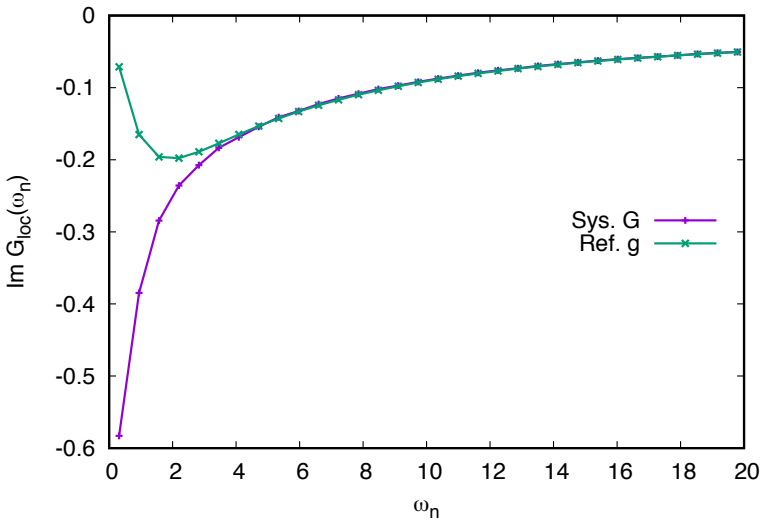

Fig. 9: *Imaginary part of the normal local Green function obtained for a* 16×16 *lattice at* β=10, t=1, *and* U=5.6 *using DF-QMC. The results are obtained for the half-filled reference* g *(green) and lattice* G *(magenta) problems, and plotted as a function of Matsubara frequency* ω_n=$(2n+1)\pi/\beta$. *The lattice problem is calculated for* t'=-0.3 *and* μ=-1.8 *(*δ=13.3% *of hole doping).*

which is nothing else but the celebrated DMFT self-consistent condition for the optimal hybridization function Δ_ω and the right hand side corresponds to the $\mathbf{k}$-sum of a lattice DMFT Green function.

As a "raw" output from this DF-QMC scheme we can present the Matsubara Green functions in Eq. (36). The result is obtained for a 16×16 periodic lattice with 64 time slices. We normally measure a DF-self energy using 10^4–10^5 QMC sweeps. In Fig. 9 we show the imaginary part of the starting Green function g, obtained for the half-filled particle-hole-symmetric ($\mu = 0$, $t' = 0$) reference problem using DQMC. The full local lattice Green function G of the final system is calculated within the DF-QMC scheme. One can see that in the high-frequency limit $\omega_n \geq 10$ the dual perturbation is very small and G almost coincides with g. However, at low-frequency the lattice Green function G shows a metallic character, while the reference Green function g extrapolates to zero at $\omega \to 0$, which corresponds to the Mott-Hubbard-Slater gap. In Fig. 5 (bottom) we show the transformation of the electronic spectral function from the half-filled (reference) case with $\mu_0 = 0$ and $t' = 0$ (left panel) to the doped system with $\mu = -1.45$ and $t' = -0.3$ (right panel). The results are calculated at the inverse temperature $\beta = 5$ using stochastic analytical continuation from Matsubara space to real energy [18]. In the Mott insulator phase, corresponding to $\delta = 0\%$ doping, one can see the formation of broad Hubbard bands around the energy $E = \pm5t$, an antiferromagnetic gap $E = \pm2t$ in the antinodal point $\mathrm{X} = (\pi, 0)$ and a shadow antiferromagnetic bands at $E \simeq -3t$ in the vicinity of the $\mathrm{M} = (\pi, \pi)$ point. Upon $\delta = 15\%$ hole doping, the spectral function changes dramatically. One can clearly see a strong effect of t' on the van Hove singularity that results in the formation of a narrow, almost flat band in the Γ-X direction and the appearance of a pseudogap near the X point, which signals the quasi-localized behavior of electrons related to the formation of fluctuating local moments. On the other hand, the spectrum remains metallic near the nodal point $(\pi/2, \pi/2)$.

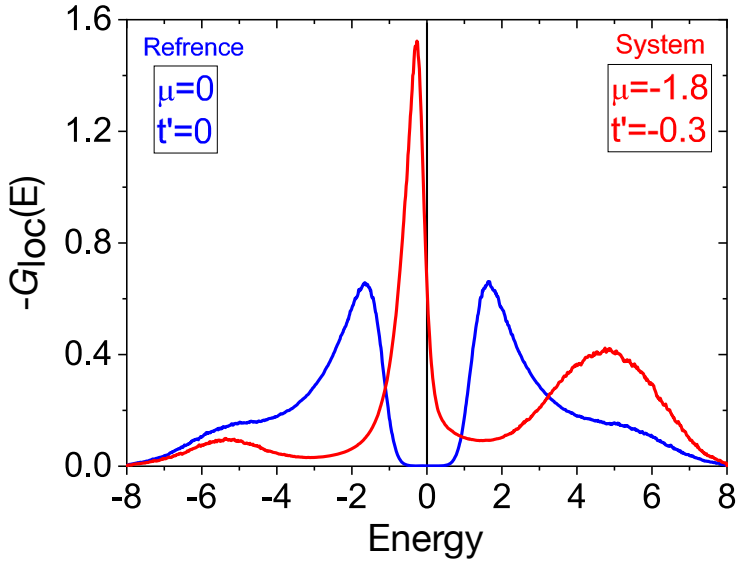

Fig. 10: *Imaginary part of the local Green function (proportional to the density of states) obtained for* $\beta = 10$ *and* $U = 5.6$ *for the half-field reference system (blue line) and the lattice problem with* $t' = -0.3$ *and* $\mu = -1.8$ *(red line), which corresponds to 13% hole doping.*

An example of the calculated the density of states or local Green function for real energies is presented in the Fig. 10 with standard t' and the μ for cuprates in comparison with the reference case. We can clearly see the formation of a narrow quasiparticle peak from the "low Slater band", while the Hubbard bands stay approximately at the same position due to the local nature of Mott-correlations. The intensity of the metallic upper Hubbard bands increases due to the "merging" with the upper Slater band.

In order to prove the convergence properties of the DF-QMC scheme we calculate the second-order contribution to the dual self-energy or the second Feynman diagram in Fig. 8. The results for lattice Green functions of the first order theory with the second order approach for a small periodic 4×4 system with relatively weak perturbations together with the exact CT-INT solution for a hole doped lattice with t' is shown in Fig. 11. There are 6 non-equivalent $\mathbf{k}$-points in the

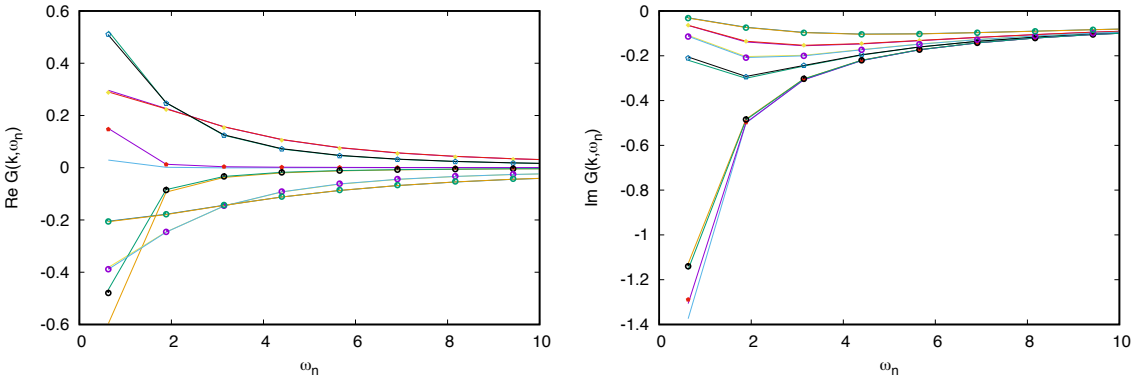

Fig. 11: *Comparison of real (left) and imaginary (right) part of the Matsubara Green functions for 6 non-equivalent* $\mathbf{k}$*-points for first and second order DF-QMC approximations (different color lines) together with exact CT-INT solution (dots) of* 4×4 *periodic system for* $U = 2$*,* $t'/t = -0.1$*,* $\mu = -0.5$ *and* $\beta = 5$*.*

Brillouin zone of the 4×4 lattice. Note that the CT-INT exact results (the dots in the Fig. 11) almost coincide with the second order DF-QMC theory and the first order scheme has small deviations (better seen for the $\mathrm{Re}\, G(\mathbf{k},\omega_0)$ part) and only for two $\mathbf{k}$-points close to the Fermi-surface: the antinodal point at $(\pi,0)$ around 0.2 and the nodal point $(\pi/2,\pi/2)$ around -0.5 on the left panel of the Fig. 11. Corresponding deviations for $\mathrm{Im}\, G(\mathbf{k},\omega_0)$ with the same color code are much smaller and the main deviation can be seen only for the antinode point (red dot in Fig. 11). All other $\mathbf{k}$-points are already converged with the first order theory. This example shows the strength and fast convergence of lattice DF-QMC expansions around the suitable reference system.

4 Dual fermions in spinor space

We can generalize the path integral DF-QMC scheme to include external magnetic or superconducting fields and investigate response of the correlated lattice model [19]. In case of an antiferromagnetic (AFM) external field in k-space $h_Q = h\,\sigma_x\delta_{k,Q}$ with $\mathrm{Q} = (\pi,\pi)$ we have a general spinor form of the perturbation

$$\tilde{t}_k(h_Q) = \begin{pmatrix} \tilde{t}_k & h_Q \\ h_Q^* & \tilde{t}_{k+Q} \end{pmatrix}. \tag{38}$$

For a d-wave superconducting field (Q=0) $\Delta_k = 2h_{dw}(\cos k_x - \cos k_y)$ the quasi-spinor perturbation in Nambu-Gor'kov space reads

$$\tilde{t}_k(h_{dw}) = \begin{pmatrix} \tilde{t}_k & \Delta_k \\ \Delta_k^* & -\tilde{t}_k^* \end{pmatrix}. \tag{39}$$

In the both case we can use the spinor form of the bare dual Green matrix in Nambu space

$$\hat{\tilde{G}} = \begin{pmatrix} \tilde{\mathcal{G}}^{\uparrow\uparrow} & \tilde{\mathcal{G}}^{\uparrow\downarrow} \\ \tilde{\mathcal{G}}^{\downarrow\uparrow} & \tilde{\mathcal{G}}^{\downarrow\downarrow} \end{pmatrix}. \tag{40}$$

The correlation effects beyond the reference problem are taken into account by the first-order contribution to the self-energy (Fig. 7) in the dual space [19]

$$\begin{aligned} \tilde{\Sigma}_{12}^{\uparrow\uparrow} &= -\sum_{3,4}\Big[\langle c_{1\uparrow}c_{2\uparrow}^*c_{3\uparrow}c_{4\uparrow}^*\rangle\,\tilde{\mathcal{G}}_{43}^{\uparrow\uparrow} + \langle c_{1\uparrow}c_{2\uparrow}^*c_{3\downarrow}c_{4\downarrow}^*\rangle\,\tilde{\mathcal{G}}_{43}^{\downarrow\downarrow}\Big], \\ \tilde{\Sigma}_{12}^{\uparrow\downarrow} &= -\sum_{3,4}\langle c_{1\uparrow}c_{2\downarrow}^*c_{3\downarrow}c_{4\uparrow}^*\rangle\tilde{\mathcal{G}}_{43}^{\uparrow\downarrow}, \end{aligned} \tag{41}$$

and similarly for the remaining two spin components. The final expression for the lattice Green function of real fermions in a superconducting external field has the following matrix form

$$\hat{G}_k = \left[\begin{pmatrix} g_k + \tilde{\Sigma}_k^{\uparrow\uparrow} & \tilde{\Sigma}_k^{\uparrow\downarrow} \\ \tilde{\Sigma}_k^{\downarrow\uparrow} & -g_k^* + \tilde{\Sigma}_k^{\downarrow\downarrow} \end{pmatrix}^{-1} - \begin{pmatrix} \tilde{t}_k & \Delta_k \\ \Delta_k^* & -\tilde{t}_k^* \end{pmatrix}\right]^{-1} \equiv \begin{pmatrix} G_k & F_k \\ F_k^* & -G_k^* \end{pmatrix}, \tag{42}$$

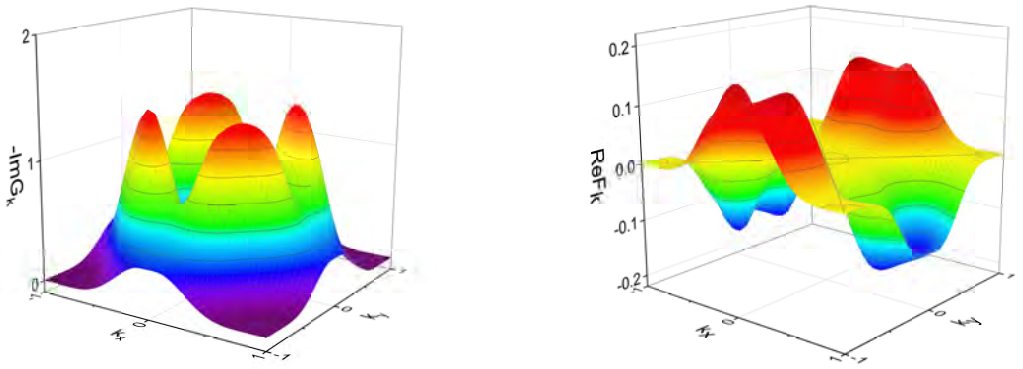

Fig. 12: *The imaginary part of the normal Green function G (left panel) and the real part of the anomalous Green function F (right panel) calculated by DF-QMC with a d-wave external field of $h_{dw} = 0.05$ at the lowest Matsubara frequency $\omega_0 = \pi/\beta$ for 12% hole doping and $\beta = 8$ for periodic 16×16 lattice [19].*

where we introduced a shortened notations for the normal $G = G^{\uparrow\uparrow}$ and anomalous $F = G^{\uparrow\downarrow}$ Green function in Nambu space. Similar spinor expressions hold for the AFM Green function.

In the Fig. 12 we plot the imaginary part of the normal Green function $G(\mathbf{k})$ (left panel), as well as the real part of the anomalous Green function $F(\mathbf{k})$ (right panel). The results are obtained at the lowest Matsubara frequency $\omega_0 = \pi T$ for the first Brillouin zone in the presence of a small external superconducting d-wave field with the amplitude $h_{dw} = 0.05$. These calculations clearly capture the formation of a large pseudogap in the electronic spectral function $-\frac{1}{\pi}\,\mathrm{Im}\,G(\mathbf{k})$ at the antinodal $\mathrm{X} = (\pi, 0)$ point, which exists already at relatively high temperatures $\beta = 5$ corresponding to $T \simeq 700\,\mathrm{K}$ for the realistic hopping amplitude $t = 0.3\,\mathrm{eV}$. Additionally, we found that the anomalous Green function $F(\mathbf{k})$ is relatively large and has a very unusual shape. Indeed, $\mathrm{Re}\,F(\mathbf{k})$ features a suppressed spectral weight at the X points, related to a pseudogap formation in the spectral function, which shifts its extrema in the direction of the nodal point.

In order to investigate connection of the pseudogap effects with the coherence properties of fermions at the antinodal X-point with $\mathbf{k} = (0, \pi)$ we calculate the imaginary part of the normal Matsubara Green function ($\mathrm{Im}\,G_k$) within DF-QMC at the anti-nodal point for a relatively high temperature $\beta = 5$ and different chemical potentials, which correspond to an underdoped system with $\delta = 2 - 9\%$, optimal doping $\delta = 10 - 18\%$, and overdoping with $\delta = 20 - 25\%$ (the left panel of the Fig. 13). It is useful to take the normalized trace of the Gor'kov Green function $(G_k - G_{-k})/2$ which just means the particle-hole symmetry with the same ($\mathrm{Im}\,G_k$) and ($\mathrm{Re}\,G_k$=0). Using this Green function, we perform a stochastic analytical continuation to real energy (right panel of the Fig. 13). We can clearly seen the complicated transformation of the pseudogap spectral function for fermions at the X-point in the underdoped system to more coherent fermions in the optimally doped case with a DMFT-like three peak structure, and finally to almost normal sharp correlated quasiparticles in the overdoped case.

We would also like to discuss the dependence of the superconducting enhancement on hole doping. For these calculations we consider a 8×8 periodic lattice with a "bare" fermionic bath,

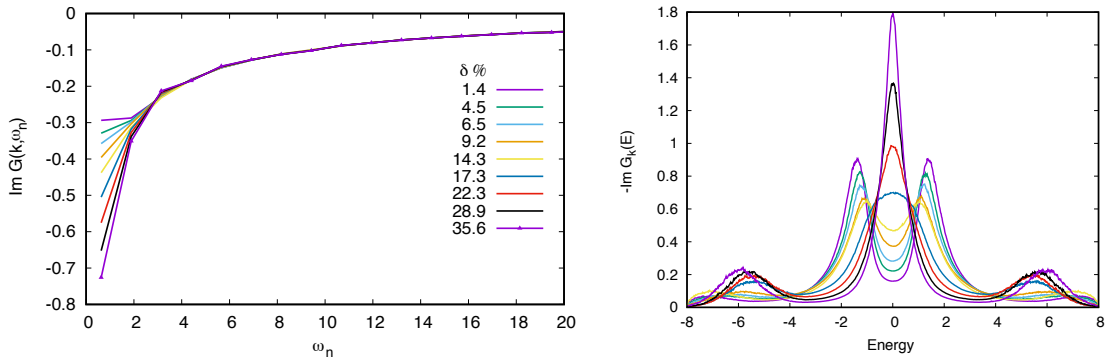

Fig. 13: *The imaginary part of the normal Green function for periodic a* 16×16 *lattice on the Matsubara axis* $\nu_n = (2n+1)\pi/\beta$ *(left panel) obtained in DF-QMC for* $\beta = 5$, $t = 1$, $t' = -0.3$ *and* $U = 5.6$ *and different chemical potentials* $-\omega = (0.8, 1.1, 1.2, 1.3, 1.45, 1.5, 1.6, 1.7, 1.8)$ *which correspond to the hole dopings shows with different colors. Corresponding analytical continuations using a SOM-scheme to the real axis* $-\operatorname{Im} G_k(E)$ *with the same color-scheme (right panel) for the* $\mathbf{k} = \mathrm{X} = (0, \pi)$.

which is introduced to reduce effects of the finite spectrum of small a system. In Fig. 14 we plot the d-wave enhancement of the anomalous Green function (F) normalized by the external superconducting field (h_{dw}) calculated at the X point, as a function of hole doping for the two values of the NNN hopping ($t' = -0.3$ and $t' = 0$). Remarkably, the dome-like superconducting behavior is found only for $t' \neq 0$. Moreover, the maximal superconducting enhancement around $\delta = 15\%$ corresponds to $\mu = -1.4$, which is very close to the position of the van Hove singularity $4t' = -1.2$ in the non-interacting spectrum. The increase of the superconducting enhancement at $\delta = 15\%$ for the optimal second-neighbor hopping $t' = -0.3$ compared to $t' = 0$ is about a factor of two. Note that in the electron doped case with $t'/t = -0.3$ the superconducting response is always smaller compare to the hole one, in agreement with the general experimental knowledge.

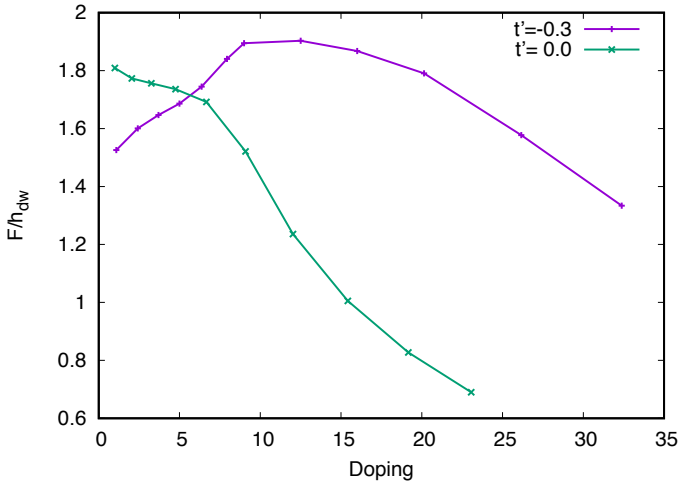

Fig. 14: *The enhancement of the anomalous Green function at the lowest Matsubara frequency* $\nu_0 = \pi/\beta$, *with respect to the external* d*-wave field* $h_{dw} = 0.05$. *The ratio of* F/h_{dw} *is calculated at the* $\mathbf{k} = \mathrm{X} = (0, \pi)$ *point for the* 8×8 *lattice at* $\beta = 10$ *using DF-QMC for the NNN hoppings* $t' = -0.3$ *(magenta) and* $t' = 0$ *(green) [19].*

5 Discussion

We developed the first-order strong-coupling dual fermion expansion for Hubbard-like correlated lattice models in the shift of the chemical potential (doping) and in the second-neighbor hopping (t'). The starting reference point corresponds to the half-filled particle-hole symmetric system which can be calculated numerically exactly, without fermionic sign problem. For the physically interesting parameter range of cuprate like systems (around 10% doping and $t'/t = -0.3$ we can obtain a reasonable Green function for a periodic 16×16 lattice for a temperature $T = 0.1t$. The formation of a pseudogap around the antinodal X-point and the nodal-antinodal dichotomy are clearly seen in the present approach.

We would like to point out a few main reasons why such a "super-perturbation" scheme works: first of all, the reference system already contains the main correlation effects which result in the four-peak structure of the density of states for the half-filled lattice Monte Carlo calculations [16]; second, the first-order strong-coupling perturbation relies on the lattice four-point vertex γ_{1234} (Eq. (30)) which is obtained numerically exactly and has all the information about the spin and charge susceptibilities of the lattice; and third, in case the perturbation or dual Green function $\tilde{G}^0_{12}$ (Eq. (28)) is relatively small, results will be reasonable. We discuss also the complicated question of convergence for such a dual-fermion perturbations and checked numerically the second-order contribution in $\tilde{\Sigma}_{12}$. For this term one needs to calculate, in lattice QMC, a six-point vertex $\gamma^{(6)}$ which is a time consuming problem. Finally, we also discuss an instability towards d-wave superconductivity, introducing symmetry-breaking fields and show the complicated structure of the anomalous Green functions.

It is worthwhile to mention that for the starting reference system we can choose not only the half-filled case, but any doped case where the sign problem is mild, so we can use the DF theory to expand this numerically exact solution to regions where the sign problem in the CT-INT or convergence of the CDet is unacceptable for direct QMC calculations.

Acknowledgements

The author acknowledges support from the European Research Council via Synergy Grant No. 854843 (the FASTCORR project) and valuable communications with Mikhail Katsnelson, Alexei Rubtsov, Sergei Iskakov, Evgeny Stepanov, Igor Krivenko, Fedor Šimkovic IV, Michel Ferrero and Riccardo Rossi.

Appendices

A Path integral for fermions

We first introduce a formalism of the path integral over fermionic fields [20]. Let us consider a simple case of a single quantum state $|i\rangle$ occupied by fermionic particles [21]. Due to the Pauli principle the many-body Hilbert space is spanned by only two orthonormal states $|0\rangle$ and $|1\rangle$. In the second quantization scheme for fermions with annihilation $\hat{c}_i$ and creation $\hat{c}_i^\dagger$ operators with anticommutation relations $\{\hat{c}_i, \hat{c}_j^\dagger\} = \delta_{ij}$ we have the following simple rules

$$\hat{c}_i\,|1\rangle = |0\rangle \quad \hat{c}_i\,|0\rangle = 0 \quad \text{and} \quad \hat{c}_i^\dagger\,|0\rangle = |1\rangle \quad \hat{c}_i^\dagger\,|1\rangle = 0\,. \tag{43}$$

Moreover, the density operator and the Pauli principle have the form

$$\hat{c}_i^\dagger \hat{c}_i\,|n\rangle = n_i\,|n\rangle \quad \text{and} \quad \hat{c}_i^2 = (\hat{c}_i^\dagger)^2 = 0\,.$$

The central object here are the so-called fermionic coherent states $|c\rangle$, which are eigenstates of annihilation operator $\hat{c}_i$ with eigenvalue c_i

$$\hat{c}_i\,|c\rangle = c_i\,|c\rangle\,. \tag{44}$$

It is worthwhile to note that such a left-eigenbasis has only annihilation operators, due to the fact that they are bounded from the below and one can rewrite one of equations from Eq. (43) in the following "eigenvalue" form

$$\hat{c}_i\,|0\rangle = 0\,|0\rangle\,.$$

Due to the anti-commutation relations for the fermionic operators the eigenvalues of coherent states c_i are so-called Grassmann numbers with the multiplication rules

$$c_i c_j = -c_j c_i \quad \text{and} \quad c_i^2 = 0\,. \tag{45}$$

It is convenient to assume that the Grassmann numbers also anti-commute with the fermionic operators

$$\{c, \hat{c}\} = \{c, \hat{c}^\dagger\} = 0\,.$$

An arbitrary function of one Grassmann variable can be represented by only the first two Taylor coefficients

$$f(c) = f_0 + f_1 c\,. \tag{46}$$

One can prove the following general many-body representation of coherent states

$$|c\rangle = e^{-\sum_i c_i \hat{c}_i^\dagger}\,|0\rangle\,. \tag{47}$$

Let us show this for the simple case of one fermionic state

$$\hat{c}\,|c\rangle = \hat{c}\big(1 - c\hat{c}^\dagger\big)\,|0\rangle = \hat{c}\big(\,|0\rangle - c\,|1\rangle\,\big) = -\hat{c}c\,|1\rangle = c\,|0\rangle = c\,|c\rangle\,. \tag{48}$$

One can also define a "left" coherent state $\langle c|$ as the left-eigenstates of creation operators $\hat{c}_i^\dagger$

$$\langle c|\, \hat{c}_i^\dagger = \langle c|\, c_i^* .$$

Note that the new eigenvalue c_i^* is just another Grassmann number, not the complex conjugate of c_i. The left coherent state can be obtained similar to Eq. (47)

$$\langle c| = \langle 0|\, e^{-\sum_i \hat{c}_i c_i^*} .$$

A general function of two Grassmann variables can, analogously to Eq. (46), be represented by only four Taylor coefficients

$$f(c^*, c) = f_{00} + f_{10} c^* + f_{01} c + f_{11} c^* c \,. \tag{49}$$

Using this expansion we can define a derivative of Grassmann variables in the natural way

$$\frac{\partial c_i}{\partial c_j} = \delta_{ij} \,.$$

One needs to be careful with the "right order" of such a derivative and remember the anti-commutation rules, i.e.,

$$\frac{\partial}{\partial c_2} c_1 c_2 = -c_1 \,.$$

For the case of the general two-variable function in Eq. (49) we have

$$\frac{\partial}{\partial c^*}\frac{\partial}{\partial c} f(c^*, c) = \frac{\partial}{\partial c^*}\big(f_{01} - f_{11} c^*\big) = -f_{11} = -\frac{\partial}{\partial c}\frac{\partial}{\partial c^*} f(c^*, c).$$

One also needs a formal definition of the integration over Grassmann variables, and the natural way consists of the following rules [22]

$$\int 1\, dc = 0 \quad \text{and} \quad \int c\, dc = 1 \,,$$

which just shows that the integration over a Grassmann variable is equivalent to differentiation

$$\int \cdots\, dc \to \frac{\partial}{\partial c} \cdots$$

The coherent states are not orthonormal and the overlap of any two such states is equal to

$$\langle c|c\rangle = e^{\sum_i c_i^* c_i}$$

which is easy to see for the case of one particle

$$\langle c|c\rangle = \big(\langle 0| - \langle 1|\, c^*\big)\big(|0\rangle - c\,|1\rangle\big) = 1 + c^* c = e^{c^* c}.$$

An important property of coherent states is the resolution of unity

$$\int dc^* \int dc\, e^{-\sum_i c_i^* c_i}\, |c\rangle\langle c| = \hat{1} = \iint dc^* dc\, \frac{|c\rangle\,\langle c|}{\langle c|c\rangle}.$$

For simplicity we demonstrate this relation only for one fermion state

$$\iint dc^* dc\, e^{-c^* c}\, |c\rangle\langle c| = \iint dc^* dc \left(1 - c^* c\right)\left(|0\rangle - c\,|1\rangle\right)\left(\langle 0| - \langle 1|\, c^*\right)$$
$$= -\iint dc^* dc\; c^* c \left(|0\rangle\langle 0| + |1\rangle\langle 1|\right) = \sum_n |n\rangle\langle n| = \hat{1}\,.$$

Matrix elements of normally ordered operators are very easy to calculate in the coherent basis by operating with $\hat{c}^\dagger$ on the states to the right and $\hat{c}$ to the left:

$$\langle c^*|\, \hat{H}(\hat{c}^\dagger, \hat{c})\, |c\rangle = H(c^*, c)\, \langle c^*|c\rangle\,. = H(c^*, c)\, e^{\sum_i c_i^* c_i} \tag{50}$$

Within the manifold of coherent states we can map the fermionic operators to the Grassmann variables $(\hat{c}_i^\dagger, \hat{c}_i) \to (c_i^*, c_i)$.
Finally, we prove the so-called "trace-formula" for arbitrary fermionic operators in normal order (in one-fermion notation)

$$\mathrm{Tr}\ \hat{O} = \sum_{n=0,1} \langle n|\, \hat{O}\, |n\rangle = \sum_{n=0,1} \iint dc^* dc\, e^{-c^* c}\, \langle n|\, c\rangle\langle c|\, \hat{O}\, |n\rangle =$$
$$= \iint dc^* dc\, e^{-c^* c} \sum_{n=0,1} \langle -c|\, \hat{O}\, |n\rangle\langle n|\, c\rangle = \iint dc^* dc\, e^{-c^* c}\, \langle -c|\, \hat{O}\, |c\rangle\,.$$

The fermionic "minus" sign in the left coherent states come from the commutation of the (c^*) and (c) coherent state in such a transformation: $\langle n|c\rangle\, \langle c|n\rangle = \langle -c|n\rangle\, \langle n|c\rangle$. One has to use the standard Grassmann rules: $c_i^* c_j = -c_j c_i^*$ and $|-c\rangle = |0\rangle + c\,|1\rangle$.
We are ready now to write the partition function for the grand-canonical quantum ensemble with $H = \hat{H} - \mu\hat{N}$ and inverse temperature β. One has to use the N-slices Trotter decomposition for the partition function in $[0, \beta)$ with imaginary time $\tau_n = n\Delta\tau = n\beta/N$ $(n = 1, \ldots, N)$, and insert N times the resolution of unity as follows

$$Z = \mathrm{Tr}\, e^{-\beta H} = \iint dc^* dc\, e^{-c^* c} \big\langle -c \big| e^{-\beta H} \big| c \big\rangle$$
$$= \int \Pi_{n=1}^N dc_n^* dc_n\, e^{-\sum_n c_n^* c_n}\, \langle c_N|\, e^{-\Delta\tau H}\, |c_{N-1}\rangle\, \langle c_{N-1}|\, e^{-\Delta\tau H}\, |c_{N-2}\rangle\, ...\, \langle c_1|\, e^{-\Delta\tau H}\, |c_0\rangle$$
$$= \int \Pi_{n=1}^N dc_n^* dc_n\, e^{-\Delta\tau \sum_{n=1}^N \left(c_n^*(c_n - c_{n-1})/\Delta\tau + H(c_n^*, c_{n-1})\right)}$$

In the continuum limit $(N \to \infty)$

$$\Delta\tau \sum_{n=1}^N \cdots \to \int_0^\beta d\tau \cdots, \qquad \frac{c_n - c_{n-1}}{\Delta\tau} \to \partial_\tau \quad \text{and} \quad \Pi_{n=0}^{N-1} dc_n^* dc_n \to \mathcal{D}\,[c^*, c]$$

with antiperiodic boundary conditions for fermionic Grassmann variables in imaginary time $c(\tau)$ and $c^*(\tau)$

$$c(\beta) = -c(0), \qquad c^*(\beta) = -c^*(0)$$

we end up in the standard path-integral formulation of the partition function

$$Z = \int \mathcal{D}\left[c^*, c\right] e^{-\int_0^\beta d\tau \left(c^*(\tau)\partial_\tau c(\tau) + H(c^*(\tau), c(\tau))\right)} \; . \tag{51}$$

It is useful to mention the general form of the Gaussian path-integral for a non-interacting "quadratic" fermionic action, which is equivalent to the Hubbard-Stratonovich transformation used in the dual-fermion derivation Eq. (22). For an arbitrary matrix M_{ij} and Grassmann vectors J_i^* and J_i one can calculate analytically the following integral

$$Z_0\left[J^*, J\right] = \int \mathcal{D}\left[c^* c\right] e^{-\sum_{i,j=1}^N c_i^* M_{ij} c_j - \sum_{i=1}^N \left(c_i^* J_i + J_i^* c_i\right)} = \det M \; e^{\sum_{i,j=1}^N J_i^* (M^{-1})_{ij} J_j} \; . \tag{52}$$

To prove this relation one needs to first change variables in order to eliminate J_i^* and J_i and expand the exponential function (only the N-th oder is non-zero)

$$e^{-\sum_{i,j=1}^N c_i^* M_{ij} c_j} = \frac{1}{N!}\left(-\sum_{i,j=1}^N c_i^* M_{ij} c_j\right)^N .$$

Finally, different permutations of c_i^* and c_j and integration over Grassmann variables will give $\det M$. As a small exercise we will check such integrals for the first two many-particle dimensions. For N=1 it is trivial

$$\int \mathcal{D}\left[c^* c\right] e^{-c_1^* M_{11} c_1} = \int \mathcal{D}\left[c^* c\right] \left(-c_1^* M_{11} c_1\right) = M_{11} = \det M$$

and for N=2 we have

$$\int \mathcal{D}\left[c^* c\right] e^{-c_1^* M_{11} c_1 - c_1^* M_{12} c_1 - c_2^* M_{21} c_1 - c_2^* M_{22} c_2} =$$

$$= \frac{1}{2!}\int \mathcal{D}\left[c^* c\right] \left(-c_1^* M_{11} c_1 - c_1^* M_{12} c_1 - c_2^* M_{21} c_1 - c_2^* M_{22} c_2\right)^2 = M_{11} M_{22} - M_{12} M_{21} = \det M.$$

For a change of variables in the path integral one uses the following transformation with unit Jacobian: $c \to c + M^{-1} J$ and

$$c^* M c + c^* J + J^* c = \left(c^* + J^* M^{-1}\right) M \left(c + M^{-1} J\right) - J^* M^{-1} J \, ,$$

which proves Eq. (52). Using the Gaussian path-integral it is very easy to calculate any correlation function for a non-interaction action (Wick-theorem)

$$\left\langle c_i c_j^* \right\rangle_0 = -\frac{1}{Z_0} \frac{\delta^2 Z_0\left[J^*, J\right]}{\delta J_i^* \, \delta J_j}\bigg|_{J=0} = M_{ij}^{-1}$$

$$\left\langle c_i c_j c_k^* c_l^* \right\rangle_0 = \frac{1}{Z_0} \frac{\delta^4 Z_0\left[J^*, J\right]}{\delta J_i^* \delta J_j^* \delta J_l \delta J_k}\bigg|_{J=0} = M_{il}^{-1} M_{jk}^{-1} - M_{ik}^{-1} M_{jl}^{-1}.$$

Corresponding bosonic path-integrals can be formulated in a similar way with complex variables and periodic boundary conditions on imaginary time. The Gaussian path-integral over bosonic fields is equal to inverse of the M-matrix determinant [20].

References

[1] E. Gull, A.J. Millis, A.I. Lichtenstein, A.N. Rubtsov, M. Troyer, and P. Werner, Rev. Mod. Phys. **83**, 349 (2011)

[2] D.M. Ceperley and B.J. Alder, Phys. Rev. Lett. **45**, 566 (1980)

[3] A. Georges, G. Kotliar, W. Krauth, and M.J. Rozenberg, Rev. Mod. Phys. **68**, 13 (1996)

[4] H. Hafermann, F. Lechermann, A. Rubtsov, M. Katsnelson, A. Georges, and A. Lichtenstein, in D.C. Cabra, A. Honecker, and P. Pujol (eds.): *Modern theories of many-particle systems in condensed matter physics* (Springer, 2012), Vol. 843, chap. 4

[5] W. Metzner and D. Vollhardt, Phys. Rev. Lett. **62**, 324 (1989)

[6] G. Rohringer, H. Hafermann, A. Toschi, A.A. Katanin, A.E. Antipov, M.I. Katsnelson, A.I. Lichtenstein, A.N. Rubtsov, and K. Held, Rev. Mod. Phys. **90**, 025003 (2018)

[7] A.N. Rubtsov, M.I. Katsnelson, and A.I. Lichtenstein, Phys. Rev. B **77**, 033101 (2008)

[8] N.V. Prokof'ev and B.V. Svistunov, Phys. Rev. Lett. **81**, 2514 (1998)

[9] A.N. Rubtsov, V.V. Savkin, and A.I. Lichtenstein, Phys. Rev. B **72**, 035122 (2005)

[10] R. Rossi, Phys. Rev. Lett. **119**, 045701 (2017)

[11] A.A. Abrikosov, L.P. Gorkov, and I.E. Dzyaloshinski: *Methods of quantum field theory in statistical physics* (Dover, New York, 1975)

[12] F. Šimkovic, R. Rossi, A. Georges, and M. Ferrero, Science **385**, eade9194 (2024)

[13] S. Brener, E.A. Stepanov, A.N. Rubtsov, M.I. Katsnelson, and A.I. Lichtenstein, Ann. Phys. **422**, 168310 (2020)

[14] R. Scalettar, R. Noack, and R. Singh, Phys. Rev. B **44**, 10502 (1991)

[15] S. Iskakov, M.I. Katsnelson, and A.I. Lichtenstein, npj Comput. Mater. **10**, 36 (2024)

[16] D. Rost, E.V. Gorelik, F. Assaad, and N. Blümer, Phys. Rev. B **86**, 155109 (2012)

[17] Pairault, S., Sénéchal, D., and A.-M.S. Tremblay, Eur. Phys. J. B **16**, 85 (2000)

[18] I. Krivenko and A.S. Mishchenko, Comput. Phys. Commun. **280**, 108491 (2022)

[19] E. Stepanov, S. Iskakov, M. Katsnelson, and A. Lichtenstein: *Superconductivity of Bad Fermions: Origin of Two Gaps in HTSC Cuprates*, arXiv:2502.08635

[20] J.W. Negele and H. Orland: *Quantum Many-particle Systems* (Westview Press, 1998)

[21] A. Kamenev: *Field Theory of Non-Equilibrium Systems* (Cambridge Univ. Press, 2011)

[22] F.A. Berezin *Method of Second Quantization* (Academic Press , New York, 1966)